



## π–π Interactions in structural stability: Role in superoxide dismutases

SRĐAN Đ. STOJANOVIĆ<sup>1</sup> and MARIO V. ZLATOVIĆ<sup>2\*</sup>#

<sup>1</sup>University of Belgrade – Institute of Chemistry, Technology and Metallurgy, Department of Chemistry, Belgrade, Serbia and <sup>2</sup>Faculty of Chemistry, University of Belgrade, Belgrade, Serbia

(Received 4 April, revised 25 May, accepted 11 June 2022)

**Abstract:** In the present work, the influences of π–π interactions in superoxide dismutase (SOD) active centers were analyzed. The majority of the aromatic residues are involved in π–π interactions. Predominant type of interacting pairs is His–His and His–Trp pairs. In addition to π–π interactions, π residues also form π-networks in SOD proteins. The π–π interactions are most favorable at the pair distance range of 5–7 Å. We observed that most of the π–π interactions shows stabilization energies in the range from −4.2 to −12.6 kJ mol<sup>−1</sup>, while the metal assisted π–π interactions showed an energy in the range from −83.7 to −334.7 kJ mol<sup>−1</sup>. Most of the π–π interacting residues were evolutionary conserved and thus probably important in maintaining the structural stability of proteins through these interactions. A high percentage of these residues could be considered as stabilization centers, contributing to the net stability of SOD proteins.

**Keywords:** superoxide dismutase; dispersive forces; catalytic site.

### INTRODUCTION

Interaction between the arene systems ( $\pi$ – $\pi$ ) has been recognized as a key stabilizing force in supramolecular chemistry, drug design, biochemistry, crystal engineering and molecular science.<sup>1–6</sup> Interactions between aromatic amino acid side chains are abundant in proteins, it has been reported and gained widespread acceptance that majority (about 60 %) of all the aromatic residues in proteins are involved in aromatic interactions and among them more than 80 % are involved in imparting stability to proteins.<sup>7,8</sup> The nature of  $\pi$ – $\pi$  interaction was primarily thought to be dispersive with notable electrostatic contribution depending on the system in question.<sup>9</sup> At the supramolecular level, the aromatic rings can interact

\* Corresponding author. E-mail: mario@chem.bg.ac.rs

# Serbian Chemical Society member.

<https://doi.org/10.2298/JSC220404052S>

in different ways: stacked arrangement (face-to-face, perfect alignment, offset, slipped, parallel displaced) and edge-to-face, T-shaped conformation.<sup>10</sup> Although  $\pi-\pi$  interactions are accepted as a weak, they still play an important role in the folding and the thermal stability of proteins.<sup>11,12</sup> The calculated  $\pi-\pi$  interaction energies of the parallel, edge-face (T-shaped) and offset stacked are  $-6.2$ ,  $-10.3$  and  $-10.4$  kJ mol<sup>-1</sup>, respectively,<sup>13</sup> and the major source of attraction is not short range (such as charge-transfer), but long-range interactions (quadrupole-quadrupole electrostatic and dispersion).<sup>14</sup> It has been suggested that the perpendicular and the parallel-displaced configurations are more common than the sandwich geometry as these, especially as the former one exposes three aromatic faces to the outside, offering greater possibility for additional interactions with other groups.<sup>15</sup> Aromatic residues show a high tendency towards forming clusters beyond the dimer, having a significant influence on protein folding, structure, and stability.<sup>2,16</sup>

The presented study expands on our previous work on the anion- $\pi$  and cation- $\pi$  interactions of SOD crystal structures by analyzing the same protein group with respect to  $\pi-\pi$  interactions, in order to better understand their stabilizing role.<sup>17,18</sup> We have focused our study at the SOD active centers and hence the  $\pi-\pi$  interactions within a protein are not considered. Results from this study might be used for understanding of structure-function relationships and can provide a new dimension of molecular recognition and self-assembly.

## EXPERIMENTAL

### *Dataset*

For this study, we used the Protein Data Bank (PDB), accessed on May 10<sup>th</sup>, 2021, at that moment listing 183,118 resolved structures.<sup>19</sup> The selection criteria for superoxide dismutase to be included in the dataset were as follows: 1) crystal structures of proteins containing E.C. Number 1.15.1.1 (superoxide dismutase) with metal were accepted; 2) theoretical model structures and NMR structures were not included (these structures were not accepted as it was difficult to define the accuracy of the ensemble of structures in terms of displacement that was directly comparable to the X-ray diffraction studies); 3) only crystal structures with the resolution of 2.0 Å or better and a crystallographic *R*-factor of 25.0 % or lower were accepted; 4) we included only representatives having at least 30 % sequence identity. After assembling the dataset, several structures containing ligands and mutant amino acids were rejected, leaving 43 proteins that were actually used as the dataset in our analysis. Hydrogen atoms were added and optimized, where needed, using the program Reduce,<sup>20</sup> with default settings. Reduce software adds hydrogen atoms to protein and/or DNA structures in standardized geometry, optimizing them to the orientations of OH, SH, NH<sub>3</sub><sup>+</sup>, Met methyls, Asn and Gln sidechain amides and His rings. Software determines best hydrogen positions by selecting the best overall score from all of the possible combinations, taking into the account single scores assigned for each individual residue and for groups containing movable protons partitioned in closed sets of local interacting networks. The PDB IDs of selected protein chain structures were as follows: 1ar5:A, 1cbj:A, 1d5n:A, 1hl5:A, 1ids:A, 1isa:A, 1kkc:A, 1luv:A, 1my6:A, 1qnn:A, 1srd:A, 1to4:A, 1unf:X, 1xre:A, 1xuq:A, 1y67:A, 1yai:A, 1yso:A, 2aqn:A,

2cw2:A, 2goj:A, 2rcv:A, 2w7w:A, 3ak2:A, 3ce1:A, 3dc6:A, 3evk:A, 3f7l:A, 3h1s:A, 3js4:A, 3lio:A, 3lsu:A, 3mds:A, 3pu7:A, 3tqj:A, 4br6:A, 4c7u:A, 4f2n:A, 4ffk:A, 4yet:A, 5a9g:A, 5vf9:A and 6bej:A.

#### $\pi$ - $\pi$ interaction analysis

A computer program Discovery Studio Visualizer 2020<sup>21</sup> was used for the calculation of various types  $\pi$ - $\pi$  interactions and their geometrical features with default settings (Fig. 1).  $\pi$ - $\pi$  interactions are determined following the methodology of McGaughey.<sup>10</sup> This method finds stacked and staggered  $\pi$ - $\pi$  interactions by performing the following tests: 1) the distance between the centroid of each pair of  $\pi$  rings is determined to find those which fall within the  $\pi$ - $\pi$  centroid ( $R_{cen}$ ) cutoff distance ( $R_{cen} < 7 \text{ \AA}$ ). For these, an atom from each ring should be within the closest atom distance ( $R_{clo}$ ) cutoff distance ( $R_{clo} < 7 \text{ \AA}$ ). The angle  $\theta$  between the normal of one or both rings and the centroid-centroid vector must fall between  $0^\circ$  and  $\pm \theta$  angle cutoff ( $\theta < 90^\circ$ ), and the angle  $\lambda$  between the normal to each ring must fall between  $0^\circ$  and  $\pm \lambda$  angle cutoff ( $\lambda < 90^\circ$ ). The aromatic systems include the aromatic side chains of the residues tryptophan (Trp), tyrosine (Tyr), phenylalanine (Phe) and histidine (His). However, as His can act either as cation or as an aromatic moiety depending on its protonation state, in our study, both the possibilities are considered.

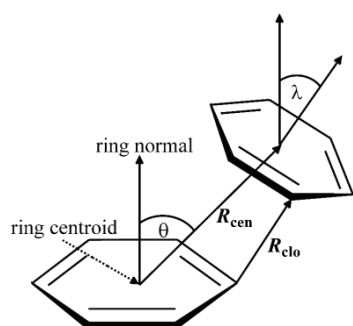


Fig. 1. Parameters for  $\pi$ - $\pi$  interactions: ( $R_{cen}$ ) the distance between the centroid of each pair of  $\pi$  rings; ( $R_{clo}$ ) the distance between the closest atom of each  $\pi$  ring; ( $\theta$ ) the angle between the normal of one or both rings and the centroid-centroid vector; and ( $\lambda$ ) the angle between the normal to each ring.

#### Computation of $\pi$ - $\pi$ interaction energy

In order to apply *ab initio* methods in determining the energies of  $\pi$ - $\pi$  pairs on desired level of theory, with sufficient level of accuracy and still in satisfactory time frame, calculations were performed on structurally reduced model systems: phenylalanine was simplified to toluene (**1**), histidine to 5-methyl-1*H*-imidazole (**2**), tryptophan to 3-methyl-1*H*-indole (**3**) and tyrosine was reduced to 4-methylphenol (**4**, Fig. 2).<sup>17</sup>

Using of reduced model of large systems in calculations of specific intramolecular interaction is well known and already proved methodology,<sup>22</sup> producing results accurate enough, and still significantly reducing computation times and strength needed for them. Larger models, like whole amino acids, or parts of protein chain, would unnecessary complicate calculations and probably even bring in the errors. Numerous interactions mechanisms are possible in a larger protein structure, and a single binding energy computation cannot always correctly determine which of these interactions are present and to what amount they contribute to overall stabilization. As a result, separating the involvement of the  $\pi$ - $\pi$  interaction and their energy contributions from the interacting pair residues involved in other noncovalent interactions is difficult.

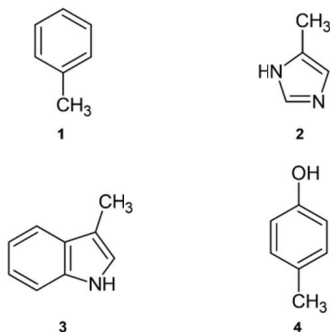


Fig. 2. Structurally reduced structures used for calculations of  $\pi-\pi$  interaction energy: 1 instead of Phe; 2 instead of His; 3 instead of Trp; 4 instead of Tyr.

*Ab initio* calculations were performed using Jaguar from Schrödinger Suite 2018-1,<sup>23</sup> using LMP2 method with triple zeta Dunning's correlation consistent basis set<sup>24</sup> and ++ diffuse functions.<sup>25</sup> All calculations were performed in vacuum. The LMP2 method applied to the study of  $\pi-\pi$  interactions, showed to be considerably faster than the MP2 method, while the calculated interaction energies and equilibrium distances were almost identical for both methods.<sup>26</sup> Several authors found that LMP2 represents an excellent method for calculation of interaction energies in proteins.<sup>27,28</sup> Sometimes, *ab initio* calculation results can be largely influenced by BSSE, and considering it is mandatory, making the calculation times significantly longer. Local correlation methods (such as LMP2) not only reduce the cost of the calculations, but the local Møller–Plesset second-order method LMP2 is well known for reducing intramolecular BSSE.<sup>29–31</sup>

Geometries of interacting structures were optimized using LMP2/cc-pVTZ(-f)++ level of theory and their single point energies calculated at LMP2/cc-pVTZ++ level. For transition metal atoms, we used the LMP2/LACVP\*\* for geometry optimization and LMP2/LACV3P\*\* for energy evaluation with effective core potentials (*ECPs*). The LACV3P basis set is a triple-contraction of the LACVP basis set,<sup>32</sup> developed and tested at Schrödinger, Inc.<sup>23</sup> Optimized geometries were placed in space to match corresponding complexes by superimposing heavy atoms onto their respective coordinates from crystal structures and then the energies of dimeric structures produced in that way were calculated.

The  $\pi-\pi$  interaction energies in dimers ( $\pi-\pi$  pairs) were calculated as the difference between the energy of the complex and the sum of the energies of the monomers in their optimized geometries. The  $\pi-\pi$  interaction energies in the ternary complex with metal were calculated as:

$$\Delta E_{\pi\pi} = E_{M\pi\pi} - (E_{M\pi} + E_\pi) \quad (1)$$

where  $E_{M\pi\pi}$ ,  $E_{M\pi}$  and  $E_\pi$  are the total energies of the ternary (metal– $\pi-\pi$ ), binary (metal– $\pi$ ) and monomeric systems ( $\pi$ ).<sup>33</sup>

#### Computation of stabilization centres

Stabilization centres (SCs) are defined as the clusters of residues making cooperative, noncovalent long-range interactions.<sup>34</sup> Measured as individual interactions, stabilisation forces resulting from noncovalent long-range interactions are not very strong, but since they are cooperative by their nature, in regions where they act in a group (SC), they could play an important role in maintaining the overall stability of protein structures. In order to analyse SC of interaction-forming residues, we used the SCide program.<sup>35</sup> The criteria SCide uses for determining SC are as follows: 1) two residues are in contact if there is, at least, one heavy atom–

–atom distance smaller than the sum of their van der Waals radii plus 1 Å; 2) a contact is recognized as “long-range” interaction if the interacting residues are, at least, ten amino acids apart; 3) two residues form a stabilization centre if they are in long-range interaction and if it is possible to select one–one residue from both flanking tetrapeptides of these two residues that make, at least, seven contacts between these two triplets.<sup>34</sup>

#### *Computation of conservation of amino acid residues*

The conservation of amino acid residues in each protein was computed using the ConSurf server.<sup>36</sup> This server computes the conservation based on the comparison of the sequence of given PDB chain with the proteins deposited in Swiss–Prot database<sup>37</sup> and identifies ones that are homologous to the PDB sequence. The number of PSI–BLAST iterations and the *E*-value cut-off used in all similarity searches were 1 and 0.001, respectively. All the sequences, evolutionary related to each one of the proteins in the dataset, were used in the subsequent multiple alignments. Based on these protein sequence alignments, the residues were classified into nine categories, from highly variable to highly conserved. Residues with a score of 1 are considered to be highly variable and residues with a score of 9 are considered to be highly conserved.

## RESULTS AND DISCUSSION

In this study, we have investigated the structural stability patterns of  $\pi$ – $\pi$  interactions in active centres of SOD proteins in relation to other environmental preferences like preference of  $\pi$ – $\pi$  interaction forming residues, interaction geometries and energetic contribution of  $\pi$ – $\pi$  interactions, stabilization centres and conservation patterns. The analyzed protein set contains 43 protein chain crystal structures and 1116  $\pi$ – $\pi$  interactions, there is an average of 26  $\pi$ – $\pi$  interactions per active center in SOD.

#### *Preference of aromatic residues for forming $\pi$ – $\pi$ interactions*

We have analyzed the frequency of occurrence of aromatic amino acid residues which are involved in  $\pi$ – $\pi$  interactions. The results are given in Table I. It can be seen that the contribution of His residue exceeds those of other three aromatic residues. The reason for this could be because, of all the aromatic amino acids, His occurs most frequently in both coordination spheres of SOD active centres.<sup>17,38</sup> The number of interactions involving other aromatic residues is similar. We compared the occurrence of interacting pairs to find the preference by SOD proteins (Table I). The highest percentage of interactions are seen between His–His pairs. Among the hetero-pairs, the occurrences of His–Trp pair are more frequent than other interacting pairs. Hence, these interactions may be quite important in the structural stability of SOD proteins.

A larger  $\pi$ -network will add more stability and play an important role in understanding the structure of proteins.<sup>39</sup> We analyzed the  $\pi$ – $\pi$  networks in these proteins as well. The analysis showed that about 73 % of the total  $\pi$ – $\pi$  interactions in the dataset are involved in the formation of multiple  $\pi$  interactions. The connectivity of  $\pi$ -ring is found to increase along the length of a network from  $2\pi$

to  $7\pi$ . A large  $\pi$ -network can enhance the stability of a protein conformation and can have a considerable influence on protein–ligand interactions. It has also been shown that addition of an aromatic pair on the protein surface increases its stability.<sup>40</sup> An illustrative example of a typical  $7\pi$ -network of cambialistic SOD from *Propionibacterium shermanii* is shown in Fig. 3.

TABLE I. Frequency of occurrence of  $\pi$ – $\pi$  interaction-forming residues in active centers of superoxide dismutase

Residue	Number of occurrences <sup>a</sup>	Occurrence <sup>b</sup> , %
His	1067	47.80
Phe	256	11.47
Trp	510	22.85
Tyr	399	17.88
Total	2232	100
Interacting pair		
His–His	344	30.82
His–Phe	64	5.73
His–Trp	204	18.28
His–Tyr	111	9.95
Phe–Phe	28	2.51
Phe–Trp	93	8.33
Phe–Tyr	43	3.85
Trp–Trp	69	6.18
Trp–Tyr	75	6.72
Tyr–Tyr	85	7.63
Total	1116	100

<sup>a</sup>The number of times a particular amino acid occurs in an appropriate interaction; <sup>b</sup>percent of amino acid occurs in an appropriate interaction

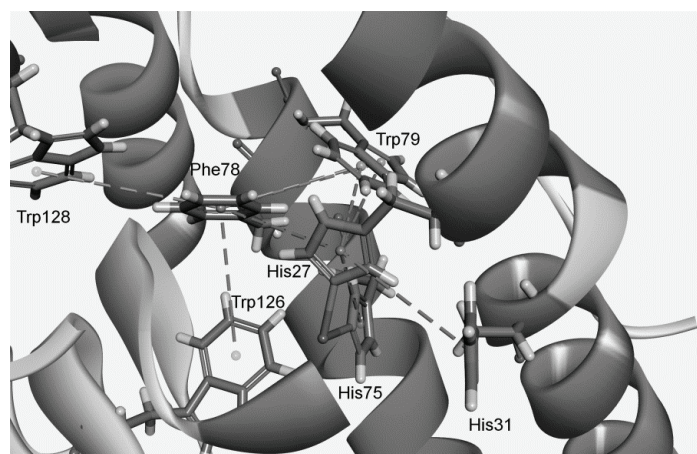


Fig. 3. Example of a multiple  $\pi$  interactions ( $\pi$ -network) for the cambialistic SOD from *Propionibacterium shermanii* (PDB code 1ar5); The interactions are marked with a dashed lines (color version is given in Supplementary material to this paper).

### Interaction geometries and energetic contribution of $\pi$ - $\pi$ interactions

On the basis of orientation of the aromatic rings, the  $\pi$ - $\pi$  interactions between two aromatic species have been broadly classified into three categories: edge to face (T-shaped), parallel displaced, and parallel stacked.<sup>41</sup> For example, McGaughey *et al.* analyzed 505 proteins and determined that an offset parallel-stacked conformation was on average 4.2 kJ mol<sup>-1</sup> more stabilizing than a T-shaped geometry.<sup>10,42</sup> We have also analyzed the frequency distribution of the distance and angle parameters of  $\pi$ - $\pi$  interacting pairs. These results are shown in

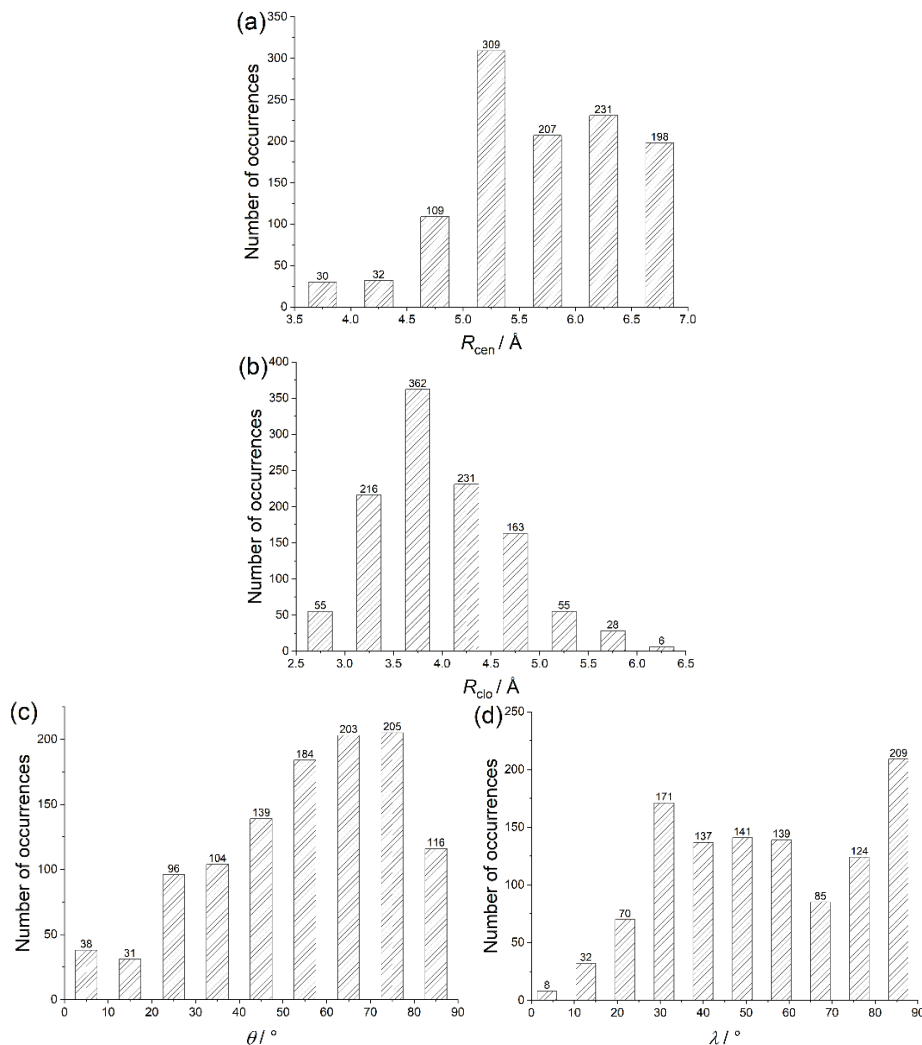


Fig. 4. Interaction geometries of  $\pi$ - $\pi$  interactions in SOD: a)  $R_{\text{cen}}$  distance distribution, b)  $R_{\text{clo}}$  distance distribution c)  $\theta$  angle distribution, d)  $\lambda$  angle distribution.

Figs. 4 and 5. The distribution of the centroid–centroid distance ( $R_{\text{cen}}$ ) for  $\pi$ – $\pi$  interactions was found to be most favorable in the distance range of 5–7 Å (Fig. 4a). This is because of T-shaped orientations having a longer  $R_{\text{cen}}$  than parallel orientations. At separation distances below 4.5 Å, aromatic pairs are rarely observed, a result of obvious physical constraints. The plot of  $R_{\text{clo}}$  distance distribution derived from  $\pi$ – $\pi$  interaction pairs (Fig. 4b), shows distribution mainly below 5.0 Å. An analysis of the plane–plane angles ( $\theta$ ) indicate that coplanarity, capable to maximizing  $\pi$ – $\pi$  stacking and packing,<sup>43</sup> was observed in relatively high number of cases (Fig. 4c). An analysis of angle  $\lambda$  showed a preference for T-shaped orientations with angles above 30° (Fig. 4d). The native structure is the compromise of a large number of noncovalent interactions that exist in proteins and the geometrical features relating two residue-types are expected to be rather broad. Overall, there was no clear overall preference for either “stacked” or “T-shaped” arrangements. For the latter, a clear orientational preference has not been determined experimentally.<sup>44,45</sup>

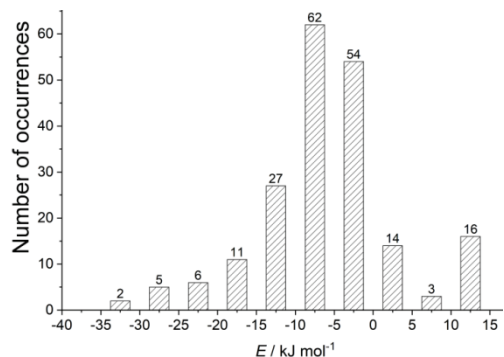


Fig. 5. Interaction energies of  $\pi$ – $\pi$  interactions in SOD.

To estimate the stabilization energy of the different  $\pi$ – $\pi$  pairs, energy calculations were carried out. To avoid calculation of more than 1000 interactions, we carefully selected 200 structures representing almost all the interactions which had been found. The results of calculations of the interaction energies for all possible interacting pairs are presented in Fig. 5.

The calculated energies range between –33.5 and 16.7 kJ mol<sup>–1</sup>, with a most populated bin in the range from –4.2 to –12.6 kJ mol<sup>–1</sup>. The energies calculated for many of the  $\pi$ – $\pi$  interactions are substantially stabilizing, with 16 % of the total showing positive (repulsive) predicted interaction energies. The repulsive nature of those interactions emerges from the unfavourable geometries of  $\pi$ – $\pi$  interactions in the crystal structures and is usually counterbalanced by other interactions.<sup>17</sup> The strongest attractive interaction (–32.7 kJ mol<sup>–1</sup>) arises for the His27–Tyr11 pair in MnSOD structure from *Escherichia coli* (PDB code 1d5n; Fig. 6a). The energies associated with  $\pi$ – $\pi$  interactions may be important contri-

butors to the overall stability of biomolecular structures and complexes and to their function through substrate binding and protein–protein interactions.

As support for the context of the  $\pi$ – $\pi$  interactions in the protein structure affecting the energetics of the system, we have analyzed the occurrence of M– $\pi$ – $\pi$  (M = Zn<sup>2+</sup>) interactions in the dataset and found 40 cation– $\pi$  interactions between Zn<sup>2+</sup> and the  $\pi$  systems of surrounding amino acids. For these ternary complexes the interaction energies are large (at least ten times larger than those calculated for individually interactions). The  $\pi$ – $\pi$  interaction energies are large and negative, ranging from –83.7 to –334.7 kJ mol<sup>–1</sup> due to the strong electrostatic effect caused by the proximity of the metal centre, thus revealing a synergistic effect between the different interactions. Quantum chemical calculations indicate that the metal ion assisted  $\pi$ – $\pi$  interaction strengths may become comparable in magnitude to that of the hydrogen bonding interaction. From our results on the interplay between cation– $\pi$  and  $\pi$ – $\pi$  interactions we suggest that these interactions can provide additional stability to the SOD proteins. Due to the presence of a great number of cation– $\pi$  and  $\pi$ – $\pi$  interactions in biological systems, this effect is important and helps to understand some biological processes where the interplay between both interactions exist. It also should be taken into account in supramolecular chemistry and crystal engineering fields.<sup>39</sup>

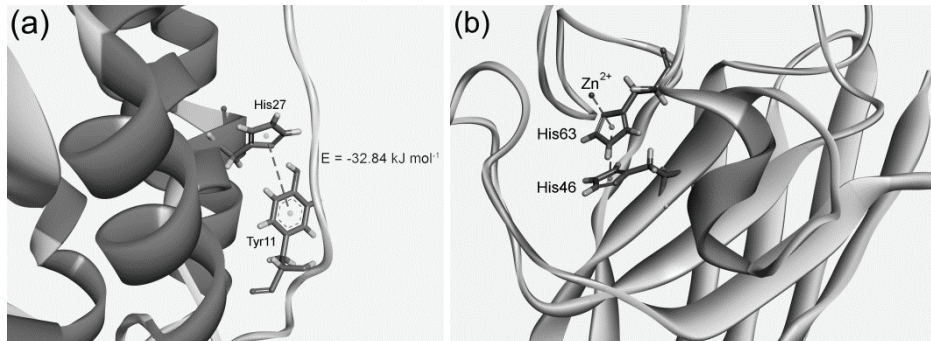


Fig. 6. Details of  $\pi$ – $\pi$  interactions: a) the strongest attractive  $\pi$ – $\pi$  interaction of *Escherichia coli* MnSOD (PDB code 1d5n). The interaction is marked with a dashed line: A:His27–A:Tyr11;  $R_{\text{cen}} = 5.70 \text{ \AA}$ ,  $R_{\text{clo}} = 3.61 \text{ \AA}$ ,  $\theta = 59.77^\circ$ ,  $\lambda = 51.92^\circ$ ,  $E = -32.7 \text{ kJ mol}^{-1}$ ; b) interaction energy of  $\pi$ – $\pi$  interaction in the presence of metal cation (Zn<sup>2+</sup>) in Cu/Zn tomato chloroplast SOD (PDB code 3pu7): A:Zn<sup>2+</sup>–A:His27–A:Tyr11;  $R_{\text{cen}} = 3.97 \text{ \AA}$ ,  $R_{\text{clo}} = 2.98 \text{ \AA}$ ,  $\theta = 26.01^\circ$ ,  $\lambda = 41.21^\circ$ ,  $E = -327.7 \text{ kJ mol}^{-1}$  (color version in SM).

In Fig. 6b, we showed structural details of the  $\pi$ – $\pi$  interaction involving transition metal ion of bovine Cu/Zn Tomato Chloroplast SOD (PDB code 3pu7). The degree of cooperativity of cation– $\pi$  and  $\pi$ – $\pi$  interaction may be quantified by comparing interaction energies in the absence of Zn<sup>2+</sup> (–19.3 kJ mol<sup>–1</sup>) and in the presence of this cation (–327.7 kJ mol<sup>–1</sup>).

*Stabilization centres and conservation of amino acid residues*

Proteins should have well-balanced stability allowing structural fluctuations and concomitantly ensuring the long-lasting equilibrium structure. Residues can be considered part of stabilization centers if they are involved in medium or long-range interactions.<sup>34</sup> We have computed the stabilization centers for all  $\pi$ - $\pi$  interaction forming residues in SOD active centers. Considering the whole data set, 45.2 % of all stabilizing residues are involved in building  $\pi$ - $\pi$  interactions. It was interesting to note that all residues involved in  $\pi$ - $\pi$  interactions were included in at least one stabilization center. These observations strongly reveal that these residues may contribute significantly to the structural stability of these proteins in addition to participating in  $\pi$ - $\pi$  interactions.

The level of evolutionary conservation was often used as an indicator for the importance of certain position in maintaining the protein's structure and/or function.<sup>46</sup> Among the  $\pi$ - $\pi$  interacting residues, 74.6 % of them showed a conservation score of higher or equal to 6. From our results we are able to infer that most of the amino acid residues involved in  $\pi$ - $\pi$  interactions might be evolutionarily conserved and might have a significant contribution to the stability of SOD proteins.

## CONCLUSION

In the present study, the analysis of the role of  $\pi$ - $\pi$  interactions in SOD proteins indicate that most of the aromatic residues are involved in  $\pi$ - $\pi$  interactions and contribute significantly to the structural stability of SOD proteins. Considering the individual contribution of aromatic residues towards  $\pi$ - $\pi$  interactions, His residues are found to have exceeded the other three aromatic amino acids. Among the interacting pairs, the His-His and His-Trp pairs have the highest frequency of occurrence than other pairs. The significant number of  $\pi$ - $\pi$  interacting residues identified in the dataset is involved in the formation of  $\pi$ -networks. We also find that all these interacting pairs are favorable in the distance range of 5–7 Å. An analysis of the plane-plane angles indicate no clear overall preference for either the “stacked” or “T-shaped” arrangements. The analysis of the energetic contribution of the protein interacting residues has revealed that most of the  $\pi$ - $\pi$  interactions have an energy in the range -4.2 to -12.6 kJ mol<sup>-1</sup>. The strongest interactions (from -83.7 to -334.7 kJ mol<sup>-1</sup>) arise for the metal assisted  $\pi$ - $\pi$  interactions. We found that, all the residues found in  $\pi$ - $\pi$  interactions are important in locating one or more stabilization centers, 45.2 % of all stabilizing residues are involved in building  $\pi$ - $\pi$  interactions, providing an additional stabilization of the SOD proteins. Moreover, the majority of the residues (74.6 %) involved in  $\pi$ - $\pi$  interactions were evolutionarily conserved. In conclusion, the results obtained from this study will be very helpful in further understanding the structural stability and functions of SOD proteins.

## SUPPLEMENTARY MATERIAL

Additional data and information are available electronically at the pages of journal website: <https://www.shd-pub.org.rs/index.php/JSCS/article/view/11744>, or from the corresponding author on request.

*Acknowledgement.* The authors would like to thank the Ministry of Education, Science and Technological Development of Republic of Serbia (Grant No: 451-03-68/2022-14/200026 and 451-03-68/2022-14/200168) for financial support.

ИЗВОД  
ИСПИТИВАЊЕ УЛОГЕ КАТЈОН- $\pi$  ИНТЕРАКЦИЈА У АКТИВНИМ ЦЕНТРИМА  
СУПЕРОКСИД-ДИСМУТАЗА

СРЂАН Ђ. СТОЈАНОВИЋ<sup>1</sup> и МАРИО В. ЗЛАТОВИЋ<sup>2</sup>

<sup>1</sup>Универзитет у Београду – Институт за хемију, технологију и металургију, Београд и <sup>2</sup>Хемијски факултет, Универзитет у Београду, Београд

У овом раду анализирани су утицаји  $\pi$ - $\pi$  интеракција у активним центрима супероксид-дисмутазе (SOD). Већина ароматичних остатака је укључена у  $\pi$ - $\pi$  интеракције. Парови His-His и His-Trp су доминантни тип парова у интеракцији. Поред  $\pi$ - $\pi$  интеракција,  $\pi$  остаци такође формирају  $\pi$ -мреже у SOD протеинима.  $\pi$ - $\pi$  интерагујући парови су најповољнији у опсегу дистанци од 5–7 Å. Приметили смо да већина  $\pi$ - $\pi$  интеракција има енергију у опсегу од -4,2 до -12,6 kJ mol<sup>-1</sup>, док су  $\pi$ - $\pi$  интеракције уз асистенцију метала показале енергију у опсегу -83,7 до -334,7 kJ mol<sup>-1</sup>. Већина  $\pi$ - $\pi$  интерагујућих остатака били су еволутивно конзервирани и могли би бити важни у одржавању структурне стабилности кроз ове интеракције. Висок проценат ових остатака може се сматрати стабилизационим центрима који доприносе нето стабилности SOD протеина.

(Примљено 4. априла, ревидирано 25. маја, прихваћено 11. јуна 2022)

## REFERENCES

1. C. D. Andersson, B. K. Mishra, N. Forsgren, F. Ekström, A. Linusson, *J. Phys. Chem., B* **124** (2020) 6529 (<https://doi.org/10.1021/acs.jpcb.0c03778>)
2. E. Lanzarotti, L. A. Defelipe, M. A. Martí, A. n. G. Turjanski, *J. Cheminf.* **12** (2020) 30 (<https://doi.org/10.1186/s13321-020-00437-4>)
3. K. S. Chatterjee, R. Das, *J. Biol. Chem.* **297** (2021) (<https://doi.org/10.1016/j.jbc.2021.100970>)
4. H. B. Gray, J. R. Winkler, *Chem. Sci.* **12** (2021) 13988 (<https://doi.org/10.1039/D1SC04286F>)
5. Z. Y. Yan, X. J. Xu, L. Fang, C. Geng, Y. P. Tian, X. D. Li, *Phytopathol. Res.* **3** (2021) 10 (<https://doi.org/10.1186/s42483-021-00088-9>)
6. S. Sasidharan, V. Ramakrishnan, *Aromatic interactions directing peptide nano-assembly. Advances in Protein Chemistry and Structural Biology*. Academic Press, Cambridge, MA, 2022 (<https://doi.org/10.1016/bs.apcsb.2022.01.001>)
7. S. K. Burley, G. A. Petsko, *Science* **229** (1985) 23 (<https://www.science.org/doi/10.1126/science.8235619>)
8. E. Cauët, M. Rooman, R. Wintjens, J. Liévin, C. Biot, *J. Chem. Theory Comput.* **1** (2005) 472 (<https://doi.org/10.1021/ct049875k>)
9. M. O. Sinnokrot, C. D. Sherrill, *J. Am. Chem. Soc.* **126** (2004) 7690 (<https://doi.org/10.1021/ja049434a>)

10. G. B. McGaughey, M. Gagné, A. K. Rappé, *J. Biol. Chem.* **273** (1998) 15458 (<https://doi.org/10.1074/jbc.273.25.15458>)
11. R. Bhattacharyya, U. Samanta, P. Chakrabarti, *Protein Eng.* **15** (2002) 91 (<https://doi.org/10.1093/protein/15.2.91>)
12. N. Kannan, S. Vishveshwara, *Protein Eng.* **13** (2000) 753 (<https://doi.org/10.1093/protein/13.11.753>)
13. S. Tsuzuki, K. Honda, T. Uchimaru, M. Mikami, K. Tanabe, *J. Am. Chem. Soc.* **124** (2002) 104 (<https://doi.org/10.1021/ja0105212>)
14. A. V. Morozov, K. M. S. Misura, K. Tsemekhman, D. Baker, *J. Phys. Chem., B* **108** (2004) 8489 (<https://doi.org/10.1021/jp037711e>)
15. C. Chipot, R. Jaffe, B. Maigret, D. A. Pearlman, P. A. Kollman, *J. Am. Chem. Soc.* **118** (1996) 11217 (<https://doi.org/10.1021/ja961379l>)
16. E. Lanzarotti, R. R. Biekofsky, D. O. A. Estrin, M. A. Marti, A. n. G. Turjanski, *J. Chem. Inf. Model.* **51** (2011) 1623 (<https://doi.org/10.1021/ci200062e>)
17. V. R. Ribić, S. Đ. Stojanović, M. V. Zlatović, *Int. J. Biol. Macromol.* **106** (2018) 559 (<https://doi.org/10.1016/j.ijbiomac.2017.08.050>)
18. S. Stojanović, M. Zlatović, *J. Serb. Chem. Soc.* **87** (2022) 465 (<https://doi.org/10.2298/JSC220109013S>)
19. P. W. Rose, B. Beran, C. Bi, W. F. Bluhm, D. Dimitropoulos, D. S. Goodsell, A. Prlic, M. Quesada, G. B. Quinn, J. D. Westbrook, J. Young, B. Yukich, C. Zardecki, H. M. Berman, P. E. Bourne, *Nucleic Acids Res.* **39** (2011) D392 (<https://doi.org/10.1093/nar/gkq1021>)
20. J. M. Word, S. C. Lovell, J. S. Richardson, D. C. Richardson, *J. Mol. Biol.* **285** (1999) 1735 (<https://doi.org/10.1006/jmbi.1998.2401>)
21. *Discovery Studio Visualizer*, Release 2020. Accelrys Software Inc., San Diego, CA
22. J. Hostaš, D. Jakubec, R. A. Laskowski, R. Gnanasekaran, J. Řezáč, J. Vondrášek, P. Hobza, *J. Chem. Theory. Comput.* **11** (2015) 4086 (<http://dx.doi.org/10.1021/acs.jctc.5b00398>)
23. *Schrödinger*, Release 2018-1: Jaguar, Schrödinger, LLC, New York, 2018
24. T. H. Dunning, *J. Chem. Phys.* **90** (1989) 1007 (<https://doi.org/10.1063/1.456153>)
25. T. Clark, J. Chandrasekhar, G. n. W. Spitznagel, P. V. R. Schleyer, *J. Comput. Chem.* **4** (1983) 294 (<https://doi.org/10.1002/jcc.540040303>)
26. A. D. Bochevarov, E. Harder, T. F. Hughes, J. R. Greenwood, D. A. Braden, D. M. Philipp, D. Rinaldo, M. D. Halls, J. Zhang, R. A. Friesner, *Int. J. Quantum Chem.* **113** (2013) 2110 (<https://doi.org/10.1002/qua.24481>)
27. K. E. Riley, J. A. Platts, J. Řezáč, P. Hobza, J. G. Hill, *J. Phys. Chem., A* **116** (2012) 4159 (<https://doi.org/10.1021/jp211997b>)
28. G. J. Jones, A. Robertazzi, J. A. Platts, *J. Phys. Chem., B* **117** (2013) 3315 (<https://doi.org/10.1021/jp400345s>)
29. S. Saebø, W. Tong, P. Pulay, *J. Chem. Phys.* **98** (1993) 2170 (<https://doi.org/10.1063/1.464195>)
30. A. Reyes, L. Fomina, L. Rumsh, S. Fomine, *Int. J. Quantum Chem.* **104** (2005) 335 (<https://doi.org/10.1002/qua.20558>)
31. R. M. Balabin, *J. Chem. Phys.* **132** (2010) 231101 (<https://doi.org/10.1063/1.3442466>)
32. P. J. Hay, W. R. Wadt, *J. Chem. Phys.* **82** (1985) 299 (<https://doi.org/10.1063/1.448975>)
33. D. Vijay, G. N. Sastry, *Chem. Phys. Lett.* **485** (2010) 235 (<https://doi.org/10.1016/j.cplett.2009.12.012>)

34. Z. Dosztányi, A. Fiser, I. Simon, *J. Mol. Biol.* **272** (1997) 597 (<https://doi.org/10.1006/jmbi.1997.1242>)
35. Z. Dosztányi, C. Magyar, G. Tusnady, I. Simon, *Bioinformatics* **19** (2003) 899 (<https://doi.org/10.1093/bioinformatics/btg110>)
36. H. Ashkenazy, E. Erez, E. Martz, T. Pupko, N. Ben-Tal, *Nucleic Acids Res.* **38** (2010) W529 (<https://doi.org/10.1093/nar/gkq399>)
37. B. Boeckmann, A. Bairoch, R. Apweiler, M. C. Blatter, A. Estreicher, E. Gasteiger, M. J. Martin, K. Michoud, C. O'Donovan, I. Phan, S. Pilbouth, M. Schneider, *Nucleic Acids Res.* **31** (2003) 365 (<https://doi.org/10.1093/nar/gkg095>)
38. S. Stojanović, Z. Petrović, M. Zlatović, *J. Serb. Chem. Soc.* **86** (2021) 781 (<https://doi.org/10.2298/JSC210321042S>)
39. A. S. Mahadevi, G. N. Sastry, *Chem. Rev.* **116** (2016) 2775 (<https://doi.org/10.1021/cr500344e>)
40. B. Ma, T. Elkayam, H. Wolfson, R. Nussinov, *Proc. Natl. Acad. Sci. USA* **100** (2003) 5772 (<https://doi.org/10.1073/pnas.1030237100>)
41. E. G. Hohenstein, C. D. Sherrill, *J. Phys. Chem., A* **113** (2009) 878 (<https://doi.org/10.1021/jp809062x>)
42. P. Chakrabarti, R. Bhattacharyya, *Prog. Biophys. Mol. Biol.* **95** (2007) 83 (<https://doi.org/10.1016/j.pbiomolbio.2007.03.016>)
43. S. Marsili, R. Chelli, V. Schettino, P. Procacci, *Phys. Chem. Chem. Phys.* **10** (2008) 2673 (<https://doi.org/10.1039/B718519G>)
44. S. Ishikawa, T. Ebata, H. Ishikawa, T. Inoue, N. Mikami, *J. Phys. Chem.* **100** (1996) 10531 (<https://doi.org/10.1021/jp960267d>)
45. A. Banerjee, A. Saha, B. K. Saha, *Crystal Growth Design* **19** (2019) 2245 (<https://doi.org/10.1021/acs.cgd.8b01857>)
46. M. Landau, I. Mayrose, Y. Rosenberg, F. Glaser, E. Martz, T. Pupko, N. Ben-Tal, *Nucleic Acids Res.* **33** (2005) W299-W302 (<https://doi.org/10.1093/nar/gki370>).